Title
Band anticrossing effects in MgyZn1-yTe1-xSex alloys

Journal
Applied Physics Letters, 80(1)

Authors
Wu, J.
Walukiewicz, W.
Yu, K.M.
et al.

Publication Date
2001-08-07

Band Anticrossing Effects in $Mg_yZn_{1-y}Te_{1-x}Se_x$ Alloys

J. Wu,

Applied Science and Technology Graduate Group, University of California, Berkeley, and

Materials Sciences Division, Lawrence Berkeley National Laboratory,

Berkeley, California 94720,

W. Walukiewicz, K.M. Yu, J.W. Ager III,

Materials Sciences Division, Lawrence Berkeley National Laboratory,

Berkeley, California 94720,

W. Shan,

OptiWork, Inc., Fremont, CA 94538,

E.E. Haller,

Department of Materials Science and Engineering, University of California, Berkeley, and

Materials Sciences Division, Lawrence Berkeley National Laboratory,

Berkeley, California 94720,

I. Miotkowski, A.K. Ramdas,

Department of Physics, Purdue University, West Lafayette, Indiana 47907

and *S. Miotkowska*

Institute of Physics, Polish Academy of Sciences, Al. Lotnikow 32/46, 02-668

Warsaw, Poland

The electronic structure of $Mg_yZn_{1-y}Te_{1-x}Se_x$ alloys were studied by optical absorption and photoluminescence techniques under applied hydrostatic pressure. In samples with both x and $y \neq 0$, the band gap exhibits a strongly nonlinear pressure dependence which is similar to the effects observed previously in $ZnTe_{1-x}Se_x$ and $ZnTe_{1-x}S_x$ ternaries and that is well explained by the anticrossing interaction of the selenium localized electronic states with the conduction band of the matrix. In contrast, the pressure dependence of the bandgap in $Mg_yZn_{1-y}Te$ (i.e. $x = 0$) is not significantly changed in form from that of ZnTe; it is concluded that the effects of alloying MgTe with ZnTe can be well understood within the virtual crystal approximation.

PACS numbers: 78.40.-q, 74.70.Dd, 78.55.Et

Electronic mail: jqwu@socrates.berkeley.edu, w_walukiewicz@lbl.gov

Quaternary alloys of the form $Mg_yZn_{1-y}Te_{1-x}Se_x$ have recently attracted considerable research attention focused on doping effects, band offsets, and lattice matching between the II-VI components involved [1]. There exists an interest in possible applications for opto-electronic devices [2], partly because their energy gaps (2.2-3.6eV) and lattice constants (5.67-6.37Å) cover wide ranges. These materials belong to a broad class of highly mismatched alloys (HMA) in which the metallic anions (Te in this case) are partially replaced by much more electronegative atoms (*i.e.*, Se). The most well-studied group of HMAs is the $IIIV_{1-x}N_x$ alloys in which the more electronegative N replaces less electronegative, more metallic As [3], P [4] or Sb [5] atoms. The electronic structure of such alloys is to a large extent determined by the interaction between the highly localized level of N and the extended states of the N-free host matrix [6-8]. In $IIIV_{1-x}N_x$ alloys the electronic structure of the conduction band near the Γ minimum is well described by a band anticrossing (BAC) model [6]. The BAC model predicts two new x-dependent subbands with dispersions produced by the hybridization of the two original states,

$$E_{\pm}(k) = \frac{1}{2}\left\{[E_M(k) + E_L] \pm \sqrt{[E_M(k) - E_L]^2 + 4xC_{LM}^2}\right\}, \qquad (1)$$

where C_{LM} is the matrix element coupling the localized and extended states, E_L is the energy of the localized level, and $E_M(k)$ is the energy of the conduction band states of the host semiconductor matrix. In alloys, $E_M(k)$ is the conduction band energy determined from an interpolation between end-point compounds within the virtual crystal approximation (VCA). In InGaAsN alloys, the two spectral signatures corresponding to E_+ and E_- have been observed and their dependencies on x and applied hydrostatic pressure have been measured and shown to be in quantitative agreement with Eq.(1) [8].

We have shown recently that the BAC model applies also to group II-VI HMAs. The composition and pressure dependence of the band gaps of $ZnTe_{1-x}S_x$ and $ZnTe_{1-y}Se_y$ alloys were measured and shown to be in agreement with Eq.(1) with the localized S and Se states located at E_S=2.6 eV and E_{Se}=2.85 eV with respect to the valence band maximum of ZnTe [9].

Here we extend these studies to $Mg_yZn_{1-y}Te$ and and $Mg_yZn_{1-y}Te_{1-x}Se_x$ alloys to determine if band anticrossing effects are found in alloys with electronegativity-mismatched cations (i.e. Mg and Zn). Also, as is seen from Eq.(1) the strength of the anticrossing interaction depends on the location of the localized level relative to the band edges of the host matrix. Quaternary alloy systems create the possibility to vary the band energies and thus the energy difference between the anion localized level and the conduction band minimum. It is important to determine the applicability of the BAC model to this system. Our results show that, indeed, for the anion mismatched systems the anticrossing interaction is entirely controlled by the location of the conduction band relative to the localized level. We also find that alloys with significant electronegativity difference on the cation sites do not show any unexpected effects and are well described within the VCA.

Single crystals of $Mg_yZn_{1-y}Te_{1-x}Se_x$ alloys with (x, y)=(8%, 10%), (0, 18.5%), and (4%, 0) were grown by the vertical gradient freezing technique. The crystals were unintentionally doped with oxygen. Details of the growth method and the alloy composition determination are described elsewhere [10]. The samples were mechanically polished into small chips with ~100×100 μm^2 in size and a thickness of ~10 μm, and mounted into gasketed diamond anvil cells for the application of hydrostatic pressure. The applied pressures were calibrated by the standard method of monitoring the red shift of the ruby R1 line.

The optical absorption measurements were performed using a 0.5m single-grating monochromator and an UV enhanced silicon photodiode. Photoluminescence (PL) signals resulted from the excitation by the 476.5nm line of an argon laser or the 325nm line of a He-Cd laser and were dispersed by a 1m double-grating monochromator.

Fig.(1) shows the optical absorption curves of $Mg_{0.10}Zn_{0.90}Te_{0.92}Se_{0.08}$ measured for a range of hydrostatic pressures. The dashed curve at the top represents a photo-modulated reflectance (PR) spectrum taken at room temperature and ambient pressure. The band gap energy determined from the PR spectrum, 2.28eV, is in agreement with the gap energy defined by the crossing point of the steeply rising portion and the saturation line of the absorption curve. The apparent absorption below the band edge originates from the fact that the reflection of the beam from the surface of the sample has been

neglected in the absorbance calculation. The relative height of the absorption curve monotonically decreases with increasing pressure, indicating a gradual degradation of the crystal quality at high pressures.

It is evident from Eq.(1) that an analysis of the experimental data in terms of the BAC model requires knowledge of the composition and pressure dependence of E_L and E_M. It has been shown previously that energies of highly localized levels remain constant on an absolute energy scale [11]. This means that their energy can be deduced from the known band offsets in a given alloy system [12].

To determine the pressure dependence of the localized level we have measured oxygen-related photoluminescence (PL) with unintentionally O-doped $ZnTe_{0.99}Se_{0.01}$. The PL spectra recorded at 30K at different hydrostatic pressures are shown in Fig.(2). The broad emission band at low energies (1.8-2.1eV) is associated with the oxygen impurity [13]. The band edge emission at higher energies with its phonon replicas is also clearly seen. The broad, smooth features at higher energies are due to impurity luminescence from the type-I diamonds in the diamond anvil cell. It is clear from Fig.(2) that the energy of the oxygen deep level shows a much weaker pressure dependence than the band edge. A linear fit yields the relation $E_{oxy} = 2.00 + 1.3\times10^{-3}P$ for the pressure dependence of the oxygen level, where the energy and the pressure are in units of eV and kbar, respectively. This pressure coefficient is quite close to the pressure coefficient of the Se localized level used in ref.9, 1.5meV/kbar, which was obtained from applying the BAC model to the pressure dependence of the band gap of $ZnTe_{1-x}Se_x$ alloys. We attribute the small positive pressure coefficient for the localized O level to the pressure induced downward shift of the valence band edge.

The theoretically calculated [14] valence band offsets ΔE_v(ZnTe/MgTe)=0.73 eV and ΔE_v(ZnTe/ZnSe)=0.76 eV and the known band gap energies of the end-point compounds were used to determine the location of the conduction band edges of the host semiconductor matrices, $E_M(0)$. Using these determinations of the composition dependence of the valence band edges, we plot in Fig.(3) the measured conduction band edge (CBE) energies relative to a common energy reference, *i.e.*, the valence band edge of ZnTe at ambient pressure. The pressure dependence of the CBE of ZnTe is well

represented by the relation $E_{ZnTe} = 2.243 + 0.0097\,P - 4.25\times10^{-5}P^2$. It is important to note that the CBE energy in $Mg_{0.185}Zn_{0.815}Te$ has nearly the same pressure dependence as that of ZnTe, showing clearly that the replacement of Zn (electronegativity X_{Zn}=1.5) with less electronegative Mg (X_{Mg}=1.2) does not strongly affect the pressure dependence of the resulting alloys. This is consistent with previously reported results that showed no bowing in the composition dependence of the band gap of $Mg_yZn_{1-y}Te$ alloys [15].

It is also clearly seen in Fig.(3) that the presence of Se in either $ZnTe_{0.96}Se_{0.04}$ or $Mg_{0.1}Zn_{0.9}Te_{0.92}Se_{0.08}$ considerably changes the pressure dependence of the CBE energies in these alloys. The observed tendency for the CBE energy to saturate at high pressures is a clear indication of an anticrossing effect between the localized Se level and the extended states of the conduction band. It is worthwhile to note that these large effects are observed for Se (X_{Se}=2.4) replacing Te (X_{Te}=2.1) anions. This is in contrast to the case of Mg replacing Zn cations where the same electronegativity difference does not produce any unusual effects. The sudden reduction of the CBE energy in $Mg_{0.1}Zn_{0.9}Te_{0.92}Se_{0.08}$ at the pressure of 85 kbar is attributed to the onset of a pressure induced phase transition, which has been observed previously in $Mg_yZn_{1-y}Te$ alloys [16].

The solid lines in Fig.(3) are BAC model based calculations using the pressure and composition dependencies of E_M and E_L discussed above. The best fit with the experiment is obtained with a coupling coefficient C_{LM}=1.1 eV and a Se localized level E_L=2.9 eV. These values are in excellent quantitative agreement with the values determined previously for $ZnTe_{1-x}Se_x$ ternaries (C_{LM}=1 eV and E_L=2.85 eV) [9]. It is important to note that, as is exemplified by the case of the E_{oxy}, the energies of the localized levels do not depend on pressure in our present energy reference, *i.e.*, with respect to the ambient-pressure valence band edge of ZnTe.

The successful, simultaneous fitting of the BAC model to both the Mg-containing and Mg-free samples with the same values of the parameters, C_{LM} and E_L, implies that, unlike alloying with ZnSe, the incorporation of MgTe into ZnTe results in a linear variation of the band edge energies that can be well described by the VCA. Thus, the change in the band gap of the quaternary alloy $Mg_yZn_{1-y}Te_{1-x}Se_x$ can be decomposed into a linear VCA alloying effect and a nonlinear BAC effect arising from the hybridization between the Se localized level and the VCA conduction band edge.

In conclusion, we have studied the pressure dependence of the band gap of $Mg_yZn_{1-y}Te_{1-x}Se_x$ alloys. For Se-containing samples, the observed reduction of the band gap and its pressure dependence can be explained accurately by the interaction of the Se-derived localized state, which lies at 2.90eV above the top of the valence band of ZnTe, with the VCA-derived conduction band of the alloys. Despite the large electronegativity difference between Mg and Zn, alloying of MgTe with ZnTe does not produce any unusual effects and the effect of the Mg incorporation can be well described within the VCA.

The work at Lawrence Berkeley Lab is part of the project on the "Photovoltaic Materials Focus Area" in the DOE Center of Excellence for the Synthesis and Processing of Advanced Materials, and was supported by the Director, Office of Science, Office of Basic Energy Sciences, Division of Materials Sciences of the U.S. Department of Energy under Contract No. DE-AC03-76SF00098. The work at Purdue University received support from the National Science Foundation Grant No. DMR98-00858.

References

[1]. J.H. Chang, H.M. Wang, M.W. Cho, H. Makino, H. Hanada, T. Yao, K. Shim, and H. Rabiz, J. Vac. Sci. Technol. B **18**(**3**), 1530(2000); H. Rabitz and K. Shim, J. Chem. Phys. **111**, 10640 (1999).

[2]. W. Fashinger, R. Krump, G. Brunthaler, S. Ferreira and H. Slitter, Appl. Phys. Lett. **65**, 3215(1994).

[3]. M. Kondow, K. Uomi, K. Hosomi, and T. Mozume, Jpn. J. Appl. Phys. **33**, L1056(1994); J. F. Geisz, D. J. Friedman, J. M Olson, S. R. Kurtz, and B. M. Keyes, J. Cryst. Growth, **195**, 401 (1998).

[4]. J. N. Baillargeon, K. Y. Cheng, G. E. Hofler, P. J. Pearah and K. C. Hsieh, Appl. Phys. Lett., **60**, 2540 (1992).

[5]. J.C. Harmand, G. Ungaro, J. Ramos, E.V.K. Rao, G. Saint-Girons, R. Teissier, G. Le Roux, L. Largeau, and G. Patriarche, J. Crystal Growth, to be published.

[6]. W. Shan *et al*., Phys. Rev. Lett. **82**, 1221 (1999); A. Linsay and E.P. O'Reilly, Solid State Commun. **112**, 443 (1999);

[7]. W. Shan, *et al*., Appl. Phys. Lett. **76**, 3251 (2000).

[8]. W. Walukiewicz *et al*., in *Proceedings of the 195th meeting of the electrochemical Society* (The Electrochemical Society, Inc., Pennington, NJ, 1999), Vol. 99-11, P.190.

[9]. W. Walukiewicz *et al*., Phys. Rev. Lett. 85, 1552 (2000).

[10]. M. J. Seong, H. Alawadhi, I. Miotkowski, A. K. Ramdas and S. Miotkowska, Phys. Rev. B **62**, 1866(2000).

[11]. D. Nolte, W. Walukiewicz, and E. E. Haller, Phys. Rev. Lett. **59**, 501(1987).

[12]. see e.g. W. Shan *et al.*, Phys. Rev. B **62**, 4211 (2001).

[13]. M. J. Seong, H. Alawadhi, I. Miotkowski, A. K. Ramdas and S. Miotkowska, Phys. Rev. B **60**, R16275(1999).

[14]. Su-Huai Wei and Alex Zunger, Appl. Phys. Lett **72**, 2011(1998).

[15]. M. J. Seong, H. Alawadhi, I. Miotkowski, A. K. Ramdas and S. Miotkowska, Solid State Commun. **112**, 329(1999).

[16]. Ting Li, Huan Luo, R.G. Greene, A.L. Ruoff, S.S. Trail, and F. J. DiSalvo Jr., Phys. Rev. Lett., **74**, 5232(1995); P.E. Van Camp, V.E. Van Doren, and J.L. Martins, Phys. Rev. B **55**, 775(1997).

Figure Captions

Fig.(1) Room-temperature optical absorbance curves of $Mg_{0.10}Zn_{0.90}Te_{0.92}Se_{0.08}$ at different hydrostatic pressures. The dashed curve at the top portion of the figure is a PR spectrum obtained at ambient pressure.

Fig.(2) Photoluminescence spectrum of an oxygen-containing $ZnTe_{0.99}Se_{0.01}$ sample at 30K at four pressures.

Fig.(3) Pressure dependencies of the conduction band edge (CBE) of four compounds with respect to the valence band edge of ZnTe at ambient pressure. The energy of the Se localized level and the no-phonon-line energy of the oxygen impurity level determined from the PL spectrum in $ZnTe_{0.99}Se_{0.01}$ are also shown. The solid curves through the data points of the two Se-containing samples represent the dependencies calculated using the BAC model and Eq.(1). The line through the data points of the ZnTe sample is a quadratic fitting. All the data points were obtained at room temperature except for the oxygen deep level data, which were taken at 30K.

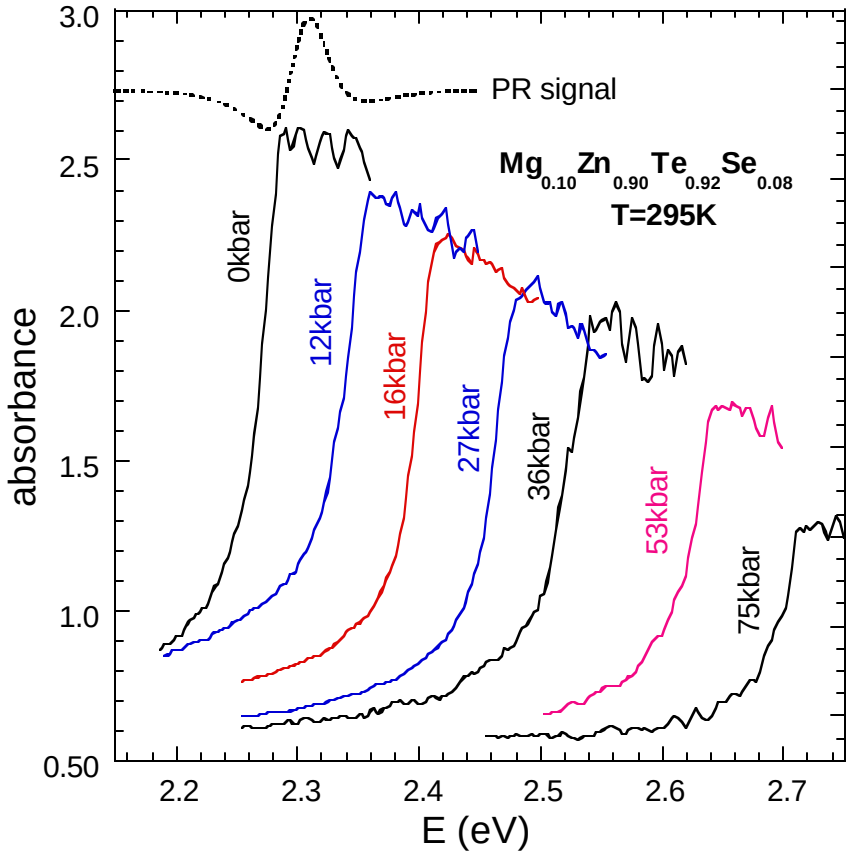
PR signal
Mg0.10Zn0.90Te0.92Se0.08
T=295K
0kbar
12kbar
16kbar
27kbar
36kbar
53kbar
75kbar
absorbance
E (eV)
3.0
2.5
2.0
1.5
1.0
0.50
2.2
2.3
2.4
2.5
2.6
2.7

Fig(1)

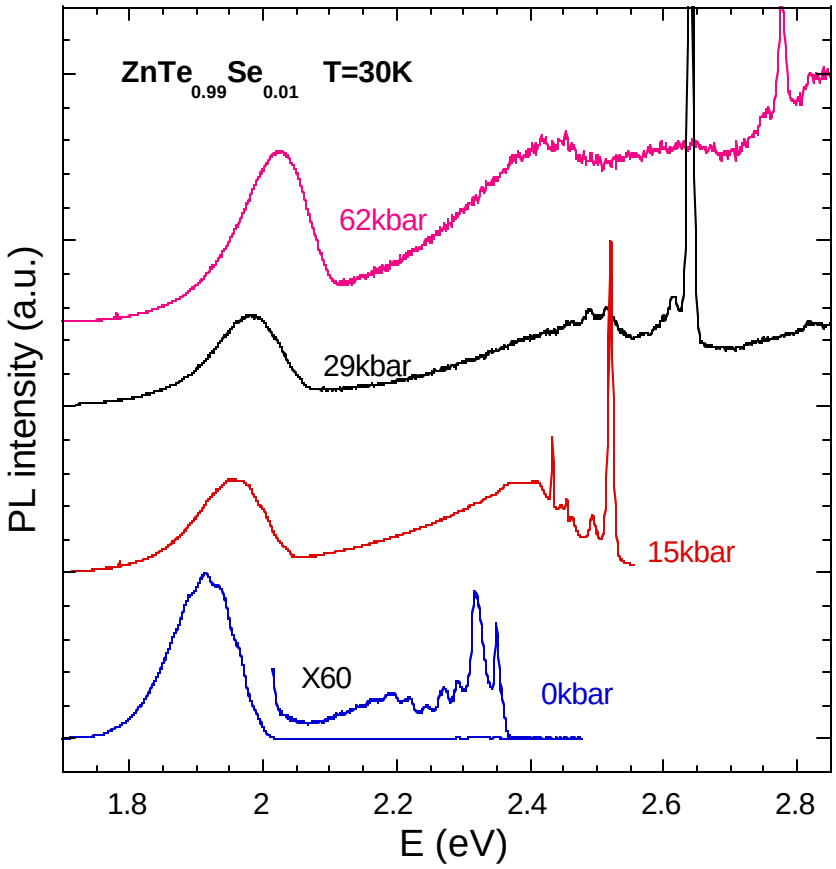
ZnTe0.99Se0.01 T=30K
62kbar
29kbar
15kbar
X60
0kbar
PL intensity (a.u.)
1.8
2
2.2
2.4
2.6
2.8
E (eV)

Fig(2)

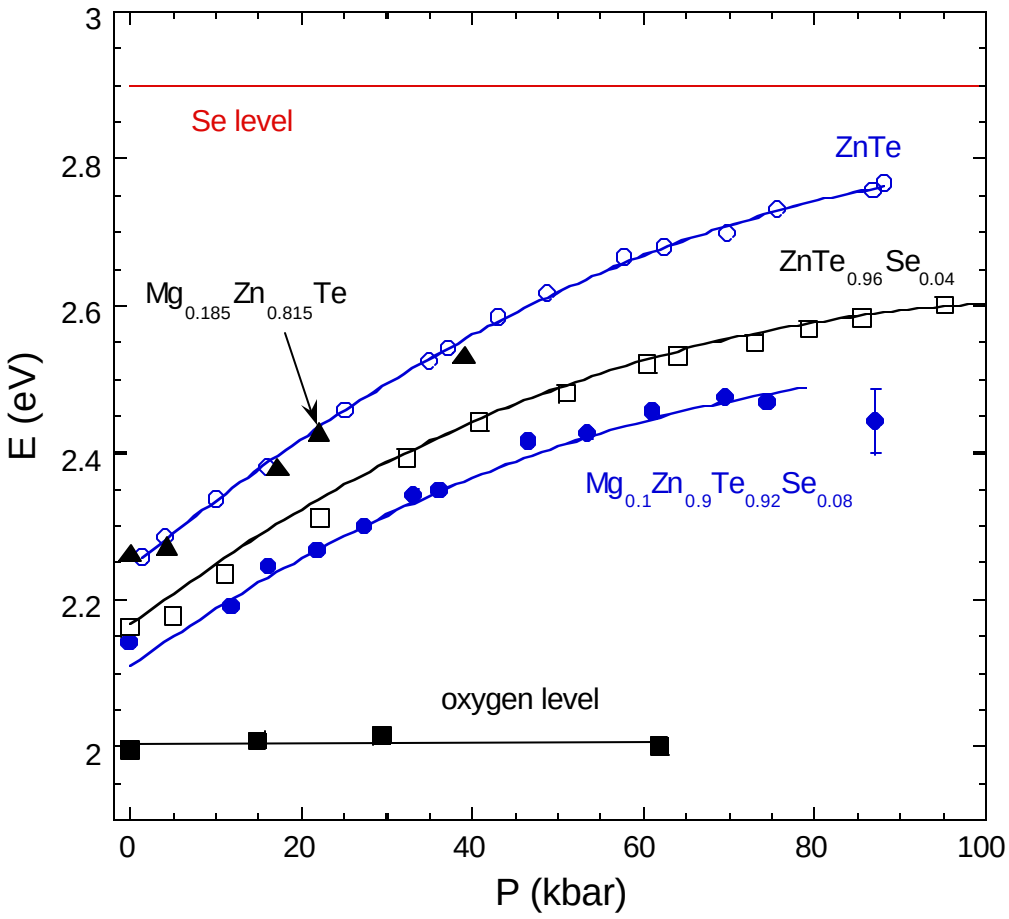
Se level
ZnTe
ZnTe0.96Se0.04
Mg0.185Zn0.815Te
Mg0.1Zn0.9Te0.92Se0.08
oxygen level
E (eV)
P (kbar)
3
2.8
2.6
2.4
2.2
2
0
20
40
60
80
100

Fig(3)